Association of Baseline Tumor-Specific Neoantigens and CD8+ T-Cell Infiltration With Immune-Related Adverse Events Secondary to Immune Checkpoint Inhibitors

Csaba Kerepesi, PhD[1]; Hassan Mohammed Abushukair, MD[2]; Biagio Ricciuti, MD[3]; Amin H. Nassar, MD[4]; Elio Adib, MD[5]; Joao V. Alessi, MD[3]; Federica Pecci, MD[3]; Mehrdad Rakaee, PhD[6]; Muhammad Zaki Hidayatullah Fadlullah, PhD[7]; Anna-Mária Tőkés, PhD[8]; Scott J. Rodig, MD, PhD[9,10]; Mark M. Awad, MD, PhD[3]; Aik Choon Tan, PhD[7]; Tibor Bakacs, MD, PhD[1]; and Abdul Rafeh Naqash, MD[11,12]

DOI https://doi.org/10.1200/PO.23.00439

ABSTRACT

PURPOSE Recent evidence has shown that higher tumor mutational burden strongly correlates with an increased risk of immune-related adverse events (irAEs). By using an integrated multiomics approach, we further studied the association between relevant tumor immune microenvironment (TIME) features and irAEs.

METHODS Leveraging the US Food and Drug Administration Adverse Event Reporting System, we extracted cases of suspected irAEs to calculate the reporting odds ratios (RORs) of irAEs for cancers treated with immune checkpoint inhibitors (ICIs). TIME features for 32 cancer types were calculated on the basis of the cancer genomic atlas cohorts and indirectly correlated with each cancer's ROR for irAEs. A separate ICI-treated cohort of non–small-cell lung cancer (NSCLC) was used to evaluate the correlation between tissue-based immune markers (CD8+, PD-1/L1+, FOXP3+, tumor-infiltrating lymphocytes [TILs]) and irAE occurrence.

RESULTS The analysis of 32 cancers and 33 TIME features demonstrated a significant association between irAE RORs and the median number of base insertions and deletions (INDEL), neoantigens (r = 0.72), single-nucleotide variant neoantigens (r = 0.67), and CD8+ T-cell fraction (r = 0.51). A bivariate model using the median number of INDEL neoantigens and CD8 T-cell fraction had the highest accuracy in predicting RORs (adjusted r^2 = 0.52, P = .002). Immunoprofile assessment of 156 patients with NSCLC revealed a strong trend for higher baseline median CD8+ T cells within patients' tumors who experienced any grade irAEs. Using machine learning, an expanded ICI-treated NSCLC cohort (n = 378) further showed a treatment duration–independent association of an increased proportion of high TIL (>median) in patients with irAEs (59.7% *v* 44%, P = .005). This was confirmed by using the Fine-Gray competing risk approach, demonstrating higher baseline TIL density (>median) associated with a higher cumulative incidence of irAEs (P = .028).

CONCLUSION Our findings highlight a potential role for TIME features, specifically INDEL neoantigens and baseline-immune infiltration, in enabling optimal irAE risk stratification of patients.

ACCOMPANYING CONTENT

Data Supplement

Accepted November 1, 2023
Published February 8, 2024

JCO Precis Oncol 8:e2300439

INTRODUCTION

The introduction of immune checkpoint inhibitors (ICIs) has revolutionized the treatment paradigm in oncology. Across numerous cancer types, ICI therapies have moved from the metastatic to the neoadjuvant/adjuvant setting.[1] ICIs, however, are often associated with a loss of tolerance to healthy self-tissues, manifesting as immune-related adverse events (irAEs). The tissue specificity, timing, and severity of irAEs vary highly and depend on the type of checkpoint inhibition and the underlying tumor type.[2] Notably, higher-grade irAEs can also lead to consequences of therapy interruptions or permanent discontinuations. Furthermore, prolonged use of immunosuppression, especially steroids, to manage irAEs can deleteriously affect the quality of life of some patients, especially older adults.

CONTEXT

Key Objective

The occurrence of immune-related adverse events (irAEs), despite being an indirect surrogate for immune checkpoint inhibitor (ICI) efficacy, frequently leads to treatment interruption and worsening patients' quality of life. In this study, we used a multiomics approach and studied the association between tumor immune microenvironment features and irAEs across 32 cancer types using a pharmacovigilance data set and an independent ICI-treated non–small-cell lung cancer (NSCLC) cohort.

Knowledge Generated

Our multiomics analyses revealed an important role for insertions and deletions neoantigens and $CD8^+$ T-cell fraction in predicting the likelihood of irAE occurrence with ICIs. Furthermore, higher baseline intratumoral presence of tumor-infiltrating lymphocytes was associated with higher irAE incidence in ICI-treated patients with NSCLC, which was independent of the duration of ICI therapy.

Relevance

Identified irAE biomarkers can provide valuable insights that could further inform patients' risk stratification for optimal ICI administration while balancing maximal efficacy and limiting toxicity.

A growing body of evidence from our group and others has demonstrated that the longitudinal development of irAEs during ICI therapies is often associated with improved outcomes with ICIs.[3-27] Ongoing efforts have centered around an integrated approach to identifying genomic, transcriptomic, and microbiome-associated predictors of irAEs.[28,29] More recently, deconvoluting the role of somatic and germline associations with irAEs is an area of emerging interest to understand the role of baseline genotypic and phenotypic features in augmenting ICI-associated irAEs among at-risk individuals. Some recent body of work has suggested an association between interleukin-7 germline variants or certain variations of human leukocyte antigen (HLA) B variants, such as HLA-B*35:01 and irAE risk.[30,31]

Among established tumor immune microenvironment (TIME) features, tumor mutational burden (TMB) has demonstrated one of the strongest correlations with irAE risk.[32] Recently, we and others have shown a significant positive correlation between the reporting odds ratios (RORs) of irAEs during ICI therapy and the corresponding TMB across 19 cancer types.[33,34] Our analysis suggested that patients with cancers harboring a high median TMB, such as melanoma and small-cell and non–small-cell lung cancers (NSCLCs), are more likely to experience irAEs secondary to ICIs. Moreover, in an ICI-treated small-cell lung cancer cohort, we previously demonstrated that patients with irAEs had a higher median TMB than patients with no reported irAEs.[35]

In this article, we extend these observations by analyzing the indirect association between the RORs of irAEs from the US Food and Drug Administration Adverse Events Reporting System (FAERS) and 33 selected TIME features across 32 cancer types on the basis of the cancer genome atlas (TCGA) using pre-existing analysis from the study by Thorsson et al.[36] Furthermore, in an independent cohort of ICI-treated patients with NSCLC who developed irAEs, using multiplexed immunofluorescence (mIF) and a machine learning approach to evaluate tumor-infiltrating lymphocytes (TILs), we evaluated baseline tumor immune phenotype composition and its association with irAEs.

METHODS

Processing FAERS Data

We downloaded the FAERS data from July 1, 2014, to December 31, 2022.[37] We excluded earlier data as primary suspect drug (PS) data were available only from the third quarter of 2014. We extracted the drugs used (including the PS medication), the indications, and the reactions for each of the 10,711,646 specific patient cases. We then performed a text search (1) in the reaction field for the terms of 105 irAEs defined by Bomze et al[34] (Data Supplement, Table S1), (2) in the indication field for cancer terms matched to 33 cancer types defined by the TCGA study and analyzed in the study by Thorsson et al[36] (Data Supplement, Table S2), and (3) in the PS drug field for the names of drugs used in ICI therapy (ipilimumab, tremelimumab, nivolumab, pembrolizumab, cemiplimab, pidilizumab, spartalizumab, tislelizumab, toripalimab, avelumab, durvalumab, and atezolizumab). Patients were included if they had been treated with anti–PD-1/anti–PD-L1 alone or with additional ICIs such as anti–cytotoxic T-cell lymphocyte antigen-4 (anti–CTLA-4). We calculated the RORs for each cancer type using a method described in Table 1. We found no cases with uterine carcinosarcoma indication when ICI drugs were applied. Thus, we considered only 32 cancer types in the further data analysis.

TABLE 1. A 2 × 2 Contingency Table for a Drug (X)-Adverse Event (Y) Combination

Drug Usage	Adverse Event (Y)	Not an Adverse Event (Y)
Using drug X	a	b
Not using drug X	c	d

NOTE. ROR = (a/b)/(c/d). The table is adapted from a previous study.[58] In our case, the drug (X) is any ICI drug and the adverse event (Y) is any irAE that occurs when a specific cancer type is the indication.
Abbreviations: ICI, immune checkpoint inhibitor; irAE, immune-related adverse event; ROR, reporting odds ratio.

Processing of Data From ClinicalTrials.gov

Data from ClinicalTrials.gov were downloaded on November 28, 2022, totaling 434,409 clinical trial records. Of the downloaded clinical trial records, 111 records were identified as having (1) completed trials with results posted, (2) where patients were administered anti–CTLA-4 (ipilimumab, tremelimumab), anti–PD-1 (nivolumab or pembrolizumab) or combination anti–PD-1 with anti–CTLA-4, and (3) trials enrolled participants with melanoma or lung cancer. We further filtered the records and identified 18,512 participants who were administered monotherapy or combination ICI therapy (Data Supplement, Table S9). On the basis of these data, we extracted the incidence of serious colitis and pneumonitis. Serious events were defined as death, a life-threatening adverse event, inpatient hospitalization or prolongation of existing hospitalization, a persistent or significant incapacity or substantial disruption of the ability to conduct normal functions, or a congenital anomaly/birth defect.

TCGA Tumor Immune Microenvironment Features

We calculated the median values for the TIME features of 32 cancer types using processed TCGA data from the study by Thorsson et al.[36] These data from the study by Thorsson et al comprised an extensive immunogenomic analysis of more than 11,000 tumors across 33 cancer types by using data compiled from the TCGA. They used immunogenomics techniques, such as assessment of the total lymphocytic infiltrate, immune cell fractions from deconvolution analysis of mRNA-seq data, immune gene expression signatures, neoantigen prediction, T-cell repertoire (TCR) and B-cell repertoire, and somatic DNA alterations. Immune cellular fraction estimates were determined by CIBERSORT (cell type identification by estimating relative subsets of RNA transcripts) applied to the TCGA RNASeq data. Potential neoantigenic peptides were identified using NetMHCpan v3.0 on the basis of HLA types derived from RNA-seq using OptiType. Somatic nonsynonymous coding single-nucleotide variants (SNVs) and somatic insertion deletion variants (INDELs) were extracted from the MC3 variant file (mc3.v0.2.8.CONTROLLED.maf) using different filters. A more detailed description of the calculation of TIME features is in the study by Thorsson et al.[39] We examined 33 TIME features (Data Supplement, Table S8). We calculated the median values for the 33 selected TIME features for 32 cancer types.

Correlation Analysis of the irAE RORs and TIME Features

After processing the FAERS database and the TCGA TIME data set in the study by Thorsson et al, we had irAE ROR values for 32 cancer types and TIME feature values for the same cancer types. For each TIME feature, we performed a separate correlation analysis. We considered cancer types only for which there were at least 100 cases of FAERS and at least 100 cases for the given TIME feature in the data set in the study by Thorsson et al. This restriction reduced the number of cancer types we examined in a specific correlation analysis. For example Figures 1B and 1E do not show melanoma (skin cutaneous melanoma [SKCM]) as there are only 83 cases for the TIME feature "INDEL Neoantigens."

Statistical Analysis

Correlations were evaluated with Pearson correlation coefficient (r) and the corresponding *P* values using the stats Pearson function of the Python package SciPy (Enthought, Austin, TX; stats module). *P* values below .05 were interpreted as significant. We used a two-sided *P* value in the study. The Benjamini-Hochberg procedure was applied for multiple hypothesis testing to control the false discovery rate (FDR; stats.multitest.function in the Python package stats models). We calculated FDR-corrected *P* values separately for the "all irAE" (Data Supplement, Table S4) and the "single irAE" analysis (Data Supplement, Table S6). The linear regression leave-one-out cross-validation method was used to construct a predictive model of ROR using TIME features with significant correlations ($P < .05$; R package caret v6.0, R Core Team, Vienna, Austria). Adjusted r-squared values were used to demonstrate each model's performance. The resulting univariate, bivariate, and trivariate models were compared using the log-likelihood ratio test (R package lmtest v0.9, lmtest developing team, Innsbruck, Austria).

Multiplexed Immunofluorescence (ImmunoProfile) From the DFCI Cohort

This approach has been previously described by the Dana-Farber Cancer Institute (DFCI) group.[39] mIF was performed on a separate cohort of NSCLCs from DFCI to determine the immunophenotype-associated subgroups by staining 5-micron formalin-fixed, paraffin-embedded whole tissue sections with standard, primary antibodies sequentially and pairing with a unique fluorochrome followed by staining with nuclear counterstain/4′,6-diamidino-2-phenylindole.[40,41] All samples were stained for PD-L1 (clone E1L3N), PD-1 (clone EPR4877[2]), CD8 (clone 4B11), and FOXP3 (clone D608R). Each sample had a single slide stained and scanned at 20× resolution using a Vectra Polaris imaging platform. Regions of interest (ROIs) were defined for each image, and only these regions were used for quantitative image analysis. inForm Image Analysis software (Perkin Elmer/Akoya, Marlborough, MA)

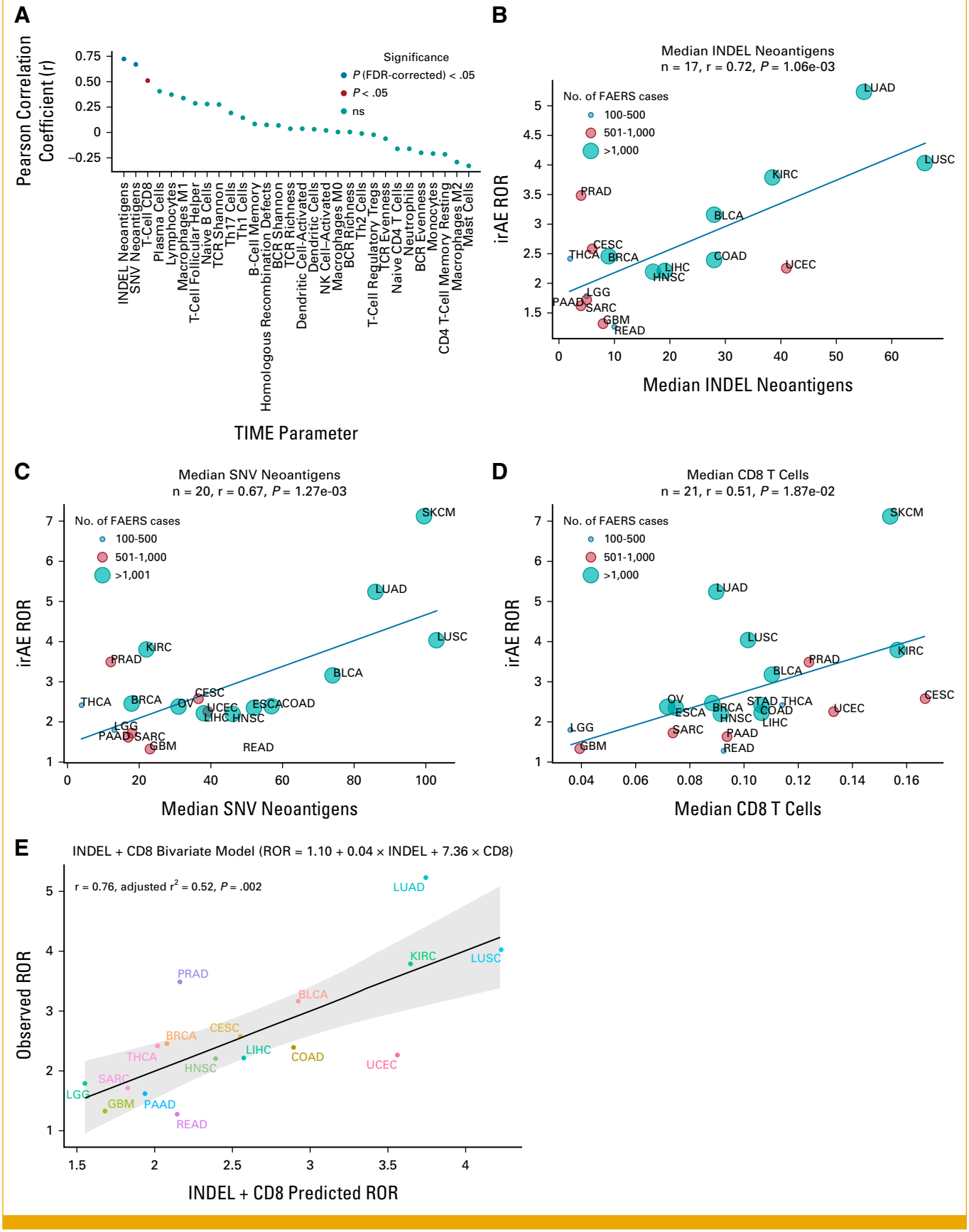

FIG 1. Associations between ROR of irAEs and TIME parameters during anti–CTLA-4, anti–PD-1, anti–PD-L1, or combination therapy. (A) Pearson correlation coefficients (r) of the irAE RORs of cancer types and median values for each examined TIME (continued on following page)

FIG 1. (Continued). feature of the same cancer types. Significance is indicated by colors. We present a detailed image for (B) INDEL neoantigens (median number of the INDEL count per case), (C) SNV neoantigens (median number of SNV neoantigen counts), and (D) $CD8^+$ T cells (median fraction of $CD8^+$ T cells). The straight lines represent the linear fit. Circle size and color represent the total number of FAERS cases for each cancer type and are shown at the top left of the figure. In the correlation analysis, we considered cancer types only for which there were at least 100 cases of FAERS and at least 100 cases in the Immune Landscape of Cancer data set. (E) Scatter plot showing the association between the predicted ROR (using the bivariate model of median INDEL neoantigens + $CD8^+$ T-cell fraction) and the observed ROR. Pearson correlation coefficients (r) and the corresponding *P* values are also shown. Anti–CTLA-4, anti–cytotoxic T-cell lymphocyte antigen-4; FAERS, Food and Drug Administration Adverse Events Reporting System; FDR, false discovery rate; INDEL, insertions and deletions; irAE, immune-related adverse event; ROR, reporting odds ratio; SNV, single-nucleotide variant; TIME, tumor immune microenvironment.

was run within each ROI to phenotype and score cells on the basis of biomarker expression. A custom script quantified the number/percentage of positive cells for relevant biomarkers in the intratumoral region, defined as the region of the slide consisting of tumors beyond the tumor-stroma interface. Cell count was calculated per ROI and averaged (unweighted) across ROIs, reported as count per millimeter squared ± standard error. Statistical significance of differential cell type enrichment between groups for the presence or absence of irAEs was estimated using the Wilcoxon rank-sum test.

Digital Pathology Assessment of TILs and Correlation With irAEs

Hematoxylin and eosin (H&E) slides were digitalized using Aperio ScanScope AT (0.49 microns/pixel; Leica Biosystems, Nußloch, Germany). Supervised machine learning algorithms (QuPath v.0.1.3; Queen's University, Belfast, Northern Ireland) were sequentially used to build an automated TIL scoring model in the following order: (1) color deconvolution to estimate the stain vectors and to normalize the RGB channels per slide as H&E intensity varied on different slides; (2) watershed segmentation to identify cells on the basis of size, shape, and optical density of nuclei in the hematoxylin layer (calculating 33 features for each cell); (3) adding intensity and smoothed object features, calculating Haralick texture features and Gaussian-weighted averages per cell; and (4) cell profiling; an object classifier was build up on the basis of the random forest algorithm to identify TILs, tumors, and stroma cells. TILs were defined as mononuclear immune cells, including lymphocytes and plasma cells. We then estimated the differences in baseline levels of TILs with the presence or absence of irAEs using the Wilcoxon rank-sum test. Logistic regression was used to adjust the association between TIL and irAE development by treatment duration.

Ethical Approval and Ethical Standards

Institutional review board approval was not required because the FAERS is an unlinkable anonymized database open to the public.

Clinicopathologic, genomic, and immunophenotypic data were collected from patients with NSCLC who had consented to institutional review board-approved correlative research protocols DF/HCC 02-180, 11-104, 13-364, and/or 17-000 at the Dana-Farber Cancer Institute (DFCI).

RESULTS

Patterns of irAEs From the FAERS Database and the ClinicalTrials.gov Data Set

We retrieved postmarketing data of adverse events from the US FAERS from July 1, 2014, to December 31, 2022, to assess the risk of developing any grade irAE (Data Supplement, Table S1) as determined by the RORs. Our search strategy identified 58,961 patients with at least one of 32 selected cancer types (Data Supplement, Table S2) who were treated with ICI-based therapy. Of these patients, 15,114 had irAEs of any grade (Fig 2A). Overall, the highest number of irAE cases occurred with SKCM, kidney renal clear cell carcinoma, and lung adenocarcinoma (LUAD) indications (Fig 2B). Serious adverse events (SAE), defined as reactions leading to death, disability, hospitalization, congenital anomalies, or an outcome requiring intervention or life-threatening, were reported in 41.2% of all 33 included cancers. The highest SAE incidence among cancers with n ≥ 1,000 was found in breast invasive carcinoma (50.6%), and the lowest (36.5%) was in renal cell carcinoma (Data Supplement, Table S7). We also reported on the incidence of specific irAEs that are either commonly associated with ICI therapy (rash, pruritus) or high morbidity/mortality (colitis, hepatitis, pneumonitis, and myocarditis[42]). Patients with cutaneous melanoma had the highest incidence of colitis (9.7%), whereas pneumonitis occurred the most in both lung squamous cell carcinoma and LUAD (4.5% and 4.4%; Data Supplement, Table S7, Fig 2C). Across the three different ICI groups associated with an irAE, the most frequently reported irAEs with anti–CTLA-4, anti–PD-1/L1, and combinational regimens were colitis (59%), rash (25%), and colitis (39%), respectively (Fig 2D).

To complement the FAERS database, we also extracted irAEs from ClinicalTrials.gov. Overall, we identified 75 clinical trials encompassing 18,512 participants with melanoma and lung cancer who were administered with single-agent anti–CTLA-4 (ipilimumab, tremelimumab) or anti–PD-1 (nivolumab, pembrolizumab) or the combination of anti–PD-1 and anti–CTLA-4. In line with observations from the FAERS database, the highest incidence of colitis (14.8%) was found in participants with melanoma, whereas pneumonitis was highest in participants with lung cancer at 9.8% (Fig 2E).

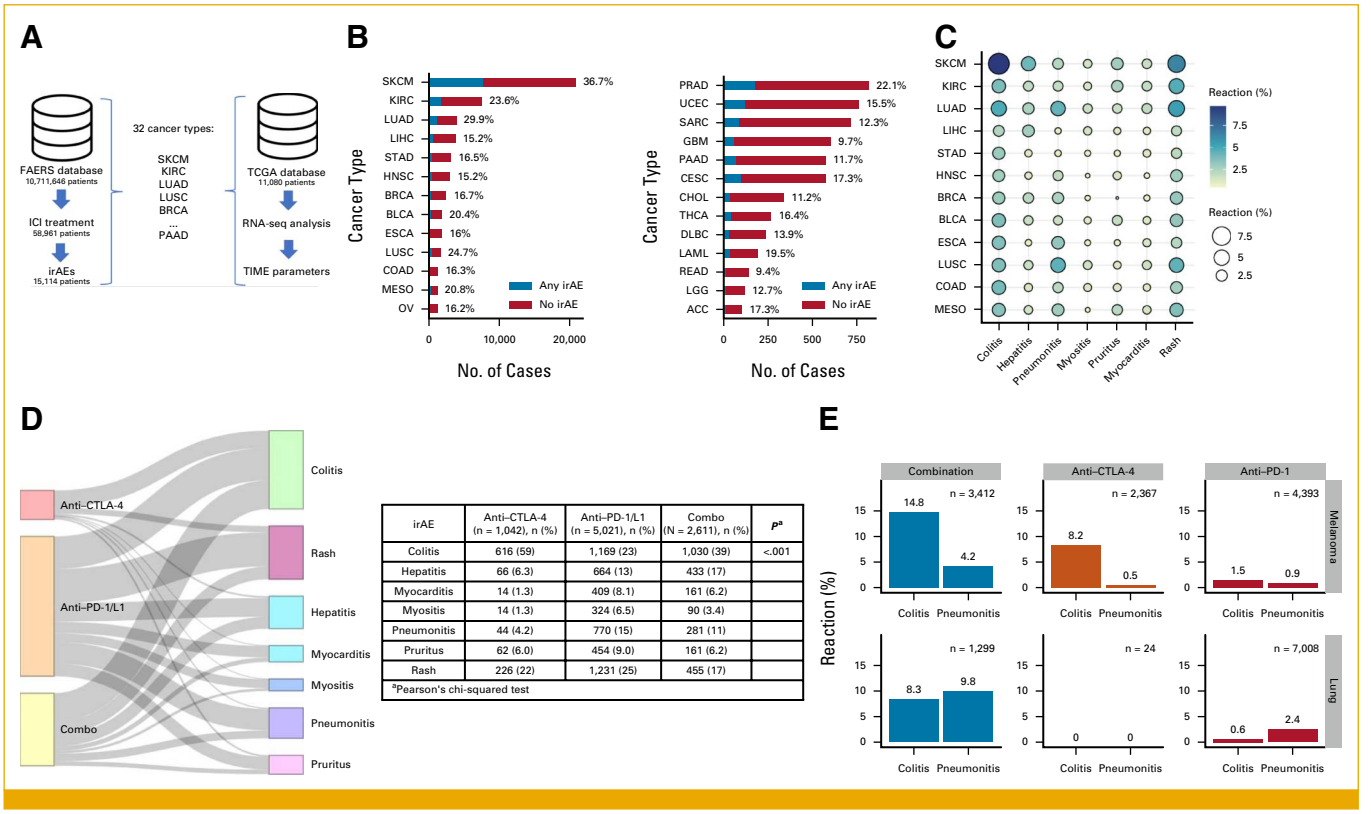

irAE	Anti–CTLA-4 (n = 1,042), n (%)	Anti–PD-1/L1 (n = 5,021), n (%)	Combo (N = 2,611), n (%)	P[a]
Colitis	616 (59)	1,169 (23)	1,030 (39)	<.001
Hepatitis	66 (6.3)	664 (13)	433 (17)	
Myocarditis	14 (1.3)	409 (8.1)	161 (6.2)	
Myositis	14 (1.3)	324 (6.5)	90 (3.4)	
Pneumonitis	44 (4.2)	770 (15)	281 (11)	
Pruritus	62 (6.0)	454 (9.0)	161 (6.2)	
Rash	226 (22)	1,231 (25)	455 (17)	

[a]Pearson's chi-squared test

FIG 2. IrAE patterns and incidence from the FAERS database. (A) Schematics of the workflow. We used two distinct databases (FAERS and TCGA) to collect irAE and TIME data (respectively), and then we examined the associations of them for 32 cancer types. (B) Number of cases with any irAE or no irAE during ICI therapy for the specific cancer types sorted by the number of total cases (left panel: cancer types with at least 1,000 cases, right panel: cancer types with cases between 100 and 1,000). Percentages of irAEs are also indicated on the right side of the bars in blue. (C) Balloon plot demonstrating the percentage of specified irAEs and each cancer type. The size and color of each circle denote percentages. (D) Alluvial plot showing the trend of irAE percentages within each ICI regimen group. (E) Bar graph depicting the percentage of irAE (pneumonitis or colitis) across the ICI treatment regimen group in melanoma (top) and lung cancer (bottom). The number of patients who were administered the treatment regimen is shown in the upper right section of the individual bar graph. Anti–CTLA-4, anti–cytotoxic T-cell lymphocyte antigen-4; FAERS, Food and Drug Administration Adverse Events Reporting System; ICI, immune checkpoint inhibitor; irAE, immune-related adverse event; TCGA, the cancer genome atlas; TIME, tumor immune microenvironment.

Specifically, the incidence of colitis increased with the use of anti–CTLA-4 versus anti–PD-1 (8.2% *v* 1.5%), whereas combinational regimens increased the frequency of both these irAEs.

TIME Features Associated With irAEs Using the FAERS and TCGA Data Set

The comparator group (no ICI used and no restriction for indications) comprised 871,582 adverse event reports from 10,711,646 patients from the FAERS database. The ROR was calculated as the odds of reporting irAEs in patients treated with anti–CTLA-4 (ipilimumab, tremelimumab), anti–PD-1 (nivolumab, pembrolizumab, cemiplimab, pidilizumab, spartalizumab, tislelizumab, toripalimab), anti–PD-L1 (avelumab, durvalumab, atezolizumab), or combination therapy (anti–PD-1 + anti–CTLA-4) divided by the odds for all other drugs in the database (Table 1).

To compare RORs with TIME features, we used an available data set generated by the Immune Landscape of Cancer study with processing RNA-seq data of the TCGA (Fig 2A). This data set contains processed data of 11,080 tumors across 33 tumor types.[36] We compared the ROR of irAEs from the FAERS with 33 selected TIME features estimated in the TCGA tumors and specifically found a significant positive correlation between irAE ROR and three features associated with antitumor immunity: the median number of insertions and deletions (INDEL) neoantigens ($r = 0.72$; $P = .0011$), the median number of SNV neoantigens ($r = 0.67$; $P = .001$), and the median $CD8^+$ T-cell fraction ($r = 0.51$; $P = .019$; Figs 1A-1D, Data Supplement, Tables S3 and S4). These three features were accordingly qualified to be included in building a more accurate composite model for ROR prediction. Using the leave-one-out cross-validation method, the bivariate model on the basis of the median number of INDEL neoantigens combined with the median $CD8^+$ T-cell fraction had the best ROR predictive performance with the highest adjusted r-squared value ($r^2 = 0.52$, $P = .002$, Fig 1E) compared with other models generated using median INDEL neoantigens, SNV neoantigens, and $CD8^+$ T cells. The resulting bivariate equation for ROR prediction was (ROR = 1.10 + 0.04 × median

INDEL neoantigens + 7.36 × $CD8^+$ T cell fraction) with 58% of ROR variability explained by a change in the median number of INDEL neoantigens and $CD8^+$ T-cell fraction. The log-likelihood ratio test showed comparable predictive performance between the bivariate model (INDEL neoantigens + $CD8^+$ T-cell fraction) and the univariate INDEL neoantigen model (P = .16).

Next, we investigated the indirect association between our specified irAEs and TIME features (Fig 3A, Data Supplement, Tables S5 and S6). The strongest correlations were found between ICI-related rash across tumor types and baseline median INDEL neoantigens (r = 0.76, P = 4.4E−04), ICI-related myocarditis across tumor types and baseline median $CD8^+$ T cells in the tumor (r = 0.68, P = .00062), and rash and $CD8^+$ T cells (r = 0.65, P = .0013). Four of the top seven correlations involved INDEL neoantigens or $CD8^+$ T cells (Figs 3B-3E). Both myocarditis and myositis were also associated with INDEL neoantigen load (r = 0.76, P = 4.37E−04; and r = 0.65, P = 5.11E−03, respectively; Fig 1A).

Immunophenotypic Characterization of Patients With NSCLC and irAEs

To further characterize the association between tumor-infiltrating immune cells and irAEs, we next analyzed an independent cohort of 156 patients with NSCLC treated with ICI from the DFCI and evaluated baseline immune cell subsets and their association with the presence or absence of irAEs. We identified a strong trend for higher baseline median $CD8^+$ T cells (P = .052; P adjusted for ICI duration = .067) before ICI treatment among patients who experienced irAEs compared with patients without irAEs (Fig 4A). These findings corroborated with our indirect analysis from the FAERS and TCGA, showing an association between baseline median $CD8^+$ T cells and irAEs across tumors. Baseline PD-L1 status (%) did not demonstrate a difference in patients with or without irAEs (P = .90, Fig 4B). To further interrogate these findings in a larger cohort, we used our previously validated machine learning approach[44] to examine potential baseline differences in TILs in patients with 378 NSCLC versus those without irAEs. We confirmed that patients who developed irAEs had significantly higher baseline median TILs compared with those without irAEs (P = .015, Fig 4C). Importantly, after adjusting for treatment duration, we confirmed a strong trend for the association between baseline TIL and irAE development (P = .07), suggesting that this correlation may potentially be independent of the duration of ICI exposure. We also analyzed the proportion of patients with versus without irAEs that had elevated TILs (>median [>338 TILs/mm^2]). We noted that patients with irAEs had a significantly higher proportion of high TILs than those without irAEs (59.7% *v* 44%, P = .005, Fig 3D). This association remained significant after adjusting for treatment duration (OR, 0.53; P = .009). We used a Fine-Gray model to estimate the cumulative incidence of irAEs, accounting for the competing risk of death. In the DFCI NSCLC cohort, high baseline TIL density (>median) was found to be associated with a higher cumulative incidence of irAEs (Fine-Gray P value = .028, Fig 4E).

DISCUSSION

Our current pan-cancer analysis revealed a significant correlation between the ROR of tumor-specific irAEs during ICI therapy and the median number of SNV neoantigens or INDEL neoantigens. In addition, we detected a positive correlation between the ROR of irAEs across tumor types and the corresponding tumor-specific median $CD8^+$ T-cell fraction. This finding was corroborated to an extent in an independent ICI-treated NSCLC cohort where patients with an irAE were noted to have a higher median $CD8^+$ T-cell infiltration. Notably, we were also able to expand on these findings using a machine learning approach on H&E slides to identify TILs and correlate these with irAEs. Furthermore, within our indirect comparison of the TCGA and the FAERS, we extended our findings and evaluated correlations between individual irAE types and TIME features. We found that some irAEs, such as myocarditis and myositis, were associated with the same TIME features (INDEL neoantigens, $CD8^+$ T cells, lymphocytes, and plasma cells), potentially suggesting a common underlying pathophysiologic mechanism, a finding that merits further investigation in future studies. Finally, our bivariate model demonstrated a strong association between the predicted ROR (using the bivariate model of median INDEL neoantigens + CD8 T-cell fraction) and the observed ROR, suggesting that a composite of these two baseline variables could help in potentially stratifying which patients may be at the highest risk for irAEs (Fig 5).

Neoantigens are foreign proteins (perturbed self) that arise from tumors through various genomic alterations (ie, SNVs, INDELs, and gene fusions) and, in turn, trigger an immune response that is not controlled by central and peripheral tolerance.[45] Among different types of genomic alterations, frameshift mutations resulting from INDELs are more likely to result in mutation-associated neoantigen generation, which creates an ideal molecular framework for antitumor T-cell immunity.[45] The correlation between the ROR of irAEs during ICI therapy with the neoantigen load and with the corresponding $CD8^+$ T-cell fraction across multiple cancer types suggests that ICIs restore the effector capacity of $CD8^+$ T cells against tumor neoantigens while breaking down tolerance against self (ie, skin rash and myocarditis). It is plausible that these irAEs from ICIs could be secondary to cross reactive neoantigens shared by tumors and distant normal tissue. The more abundant and diverse the tumor neoantigens, the more likely they will be mimicked by normal tissue neoantigens and likely result in cross-reactivity because of a clonal T-cell population, manifesting as irAEs.[46] Notably, our composite analysis for TIME features showed enhanced ROR predictive performance when factoring both median INDEL neoantigen count and $CD8^+$ T-cell fraction compared with each factor's performance alone or in combination with SNV neoantigens. Compared with SNV

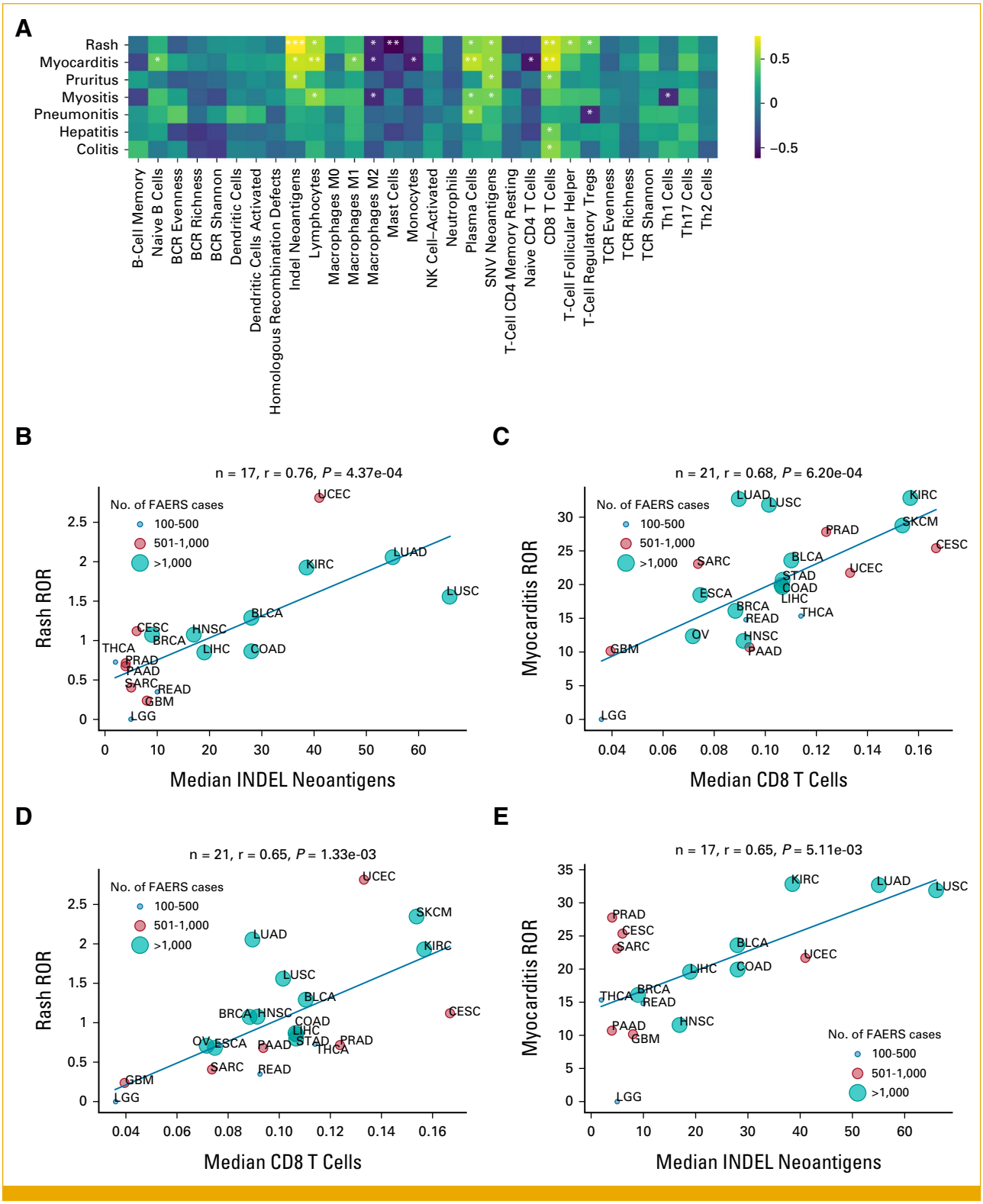

FIG 3. Associations between ROR of single irAEs and TIME parameters during anti–CTLA-4, anti–PD-1, anti–PD-L1, or combination therapy. (A) Pearson correlation coefficients (r) for the examined TIME parameters and seven specific irAEs. The significance of the correlation is indicated by asterisk (*.005 ≤ P < .05; **.0005 ≤ P < .005; ***P < .0005), (B) rash versus INDEL neoantigens, (C) myocarditis versus CD8$^+$ T cells, (D) rash versus CD8$^+$ T cells, and (E) myocarditis versus INDEL neoantigens. The straight lines represent the linear fit. Circle size and color represent the total number of FAERS cases for each cancer type and are shown at the top left of the figure. In the correlation analysis, we considered cancer types only for which there were at least 100 cases of FAERS and at least 100 cases in the Immune Landscape of Cancer data set. Pearson correlation coefficients (r) and (continued on following page)

FIG 3. (Continued). the corresponding *P* values are also shown. Anti–CTLA-4, anti–cytotoxic T-cell lymphocyte antigen-4; FAERS, Food and Drug Administration Adverse Events Reporting System; irAE, immune-related adverse event; ROR, reporting odds ratio; TIME, tumor immune microenvironment.

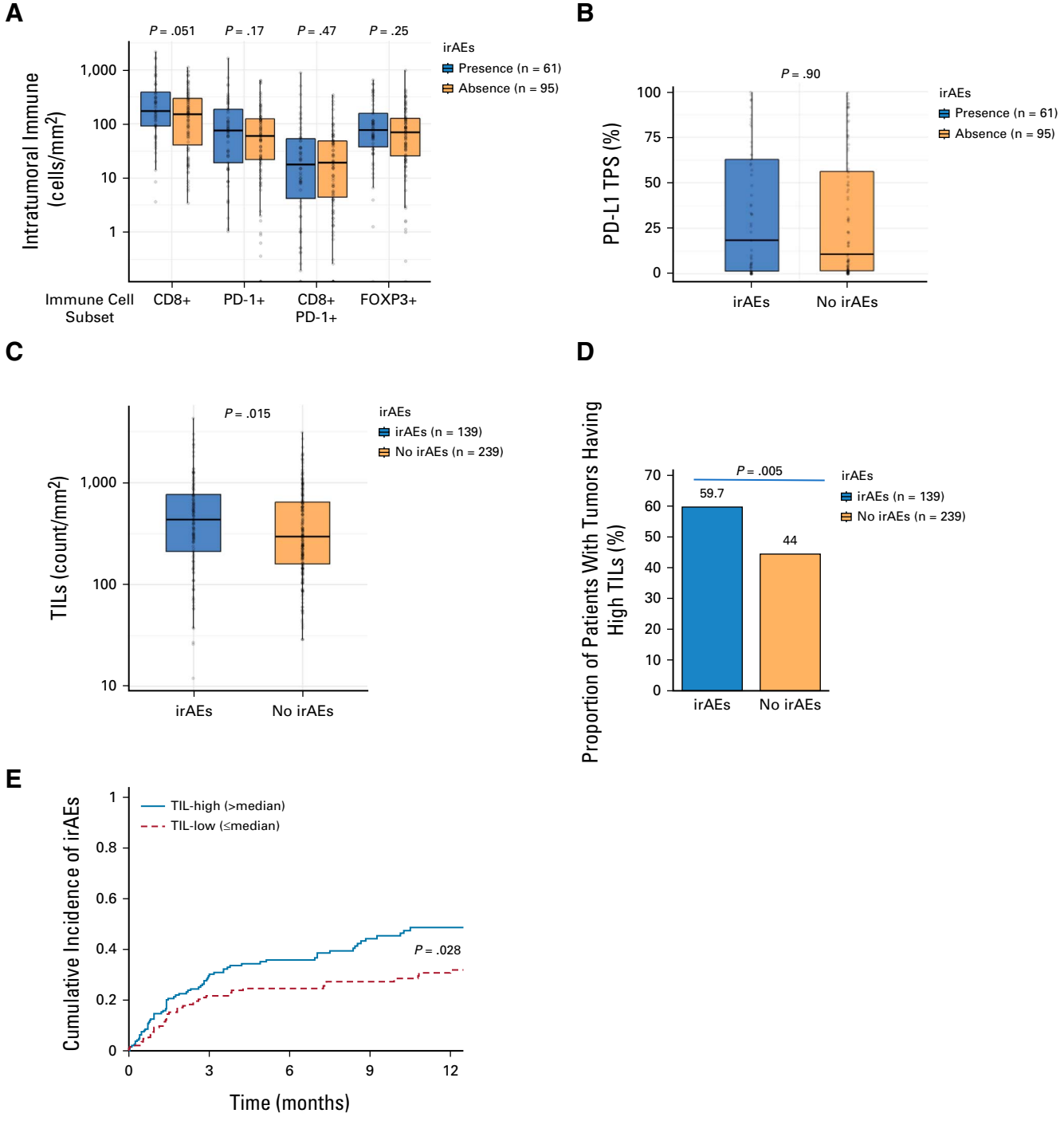

FIG 4. (A) Density of intratumoral CD8⁺, PD-1+, CD8+PD1+, and FOXP3+ cells (cells/mm²) in patients treated with the PD-(L)1 blockade with versus without irAEs. (B) PD-L1 expression levels by immunohistochemistry in patients treated with the PD-(L)1 blockade with versus without irAEs. (C) TIL density (cells/mm²) as assessed by machine learning on H&E digitalized slides. (D) Bar chart showing the proportion of patients with tumors having high (≥median) versus low (<median) TILs as assessed by machine learning in patients with versus without irAEs. (E) In the DFCI NSCLC cohort, high TIL density was found to be associated with a higher cumulative incidence of irAEs (Fine-Gray $P = .028$). DFCI, Dana-Farber Cancer Institute; H&E, Hematoxylin and Eosin; irAE, immune-related adverse event; NSCLC, non–small-cell lung cancer; TIL, tumor-infiltrating lymphocyte; TPS, tumor proportion score.

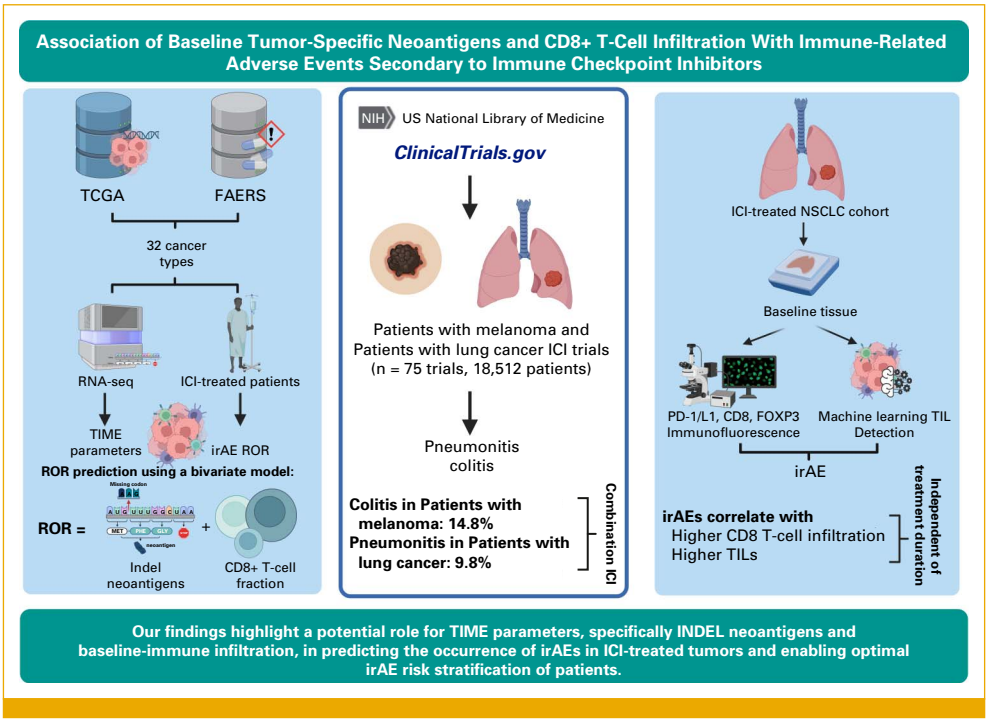

FIG 5. Association of baseline tumor-specific neoantigens and CD8$^+$ T-cell infiltration with immune-related adverse events secondary to immune checkpoint inhibitors. Created with BioRender.com. FAERS, Food and Drug Administration Adverse Events Reporting System; ICI, immune checkpoint inhibitor; INDEL, insertions and deletions; irAE, immune-related adverse event; NIH, National Institutes of Health; NSCLC, non–small-cell lung cancer; ROR, reporting odds ratio; TCGA, the cancer genome atlas; TIL, tumor-infiltrating lymphocyte; TIME, tumor immune microenvironment.

neoantigens, INDEL mutations often lead to more immunogenic mutations as one study reported that neoantigens derived from INDEL mutations were nine times more enriched for mutant-specific binding compared with nonsynonymous SNV-derived neoantigens in renal cancers.[47]

Using a similar approach, Zhang et al also analyzed large-scale pharmacovigilance data of irAEs from the FAERS and separate TCGA multiomics data. However, their analysis from the FAERS database was restricted to irAEs because of anti–PD-1 therapy only,[32] whereas our data set for ICIs is not restricted to anti–PD-1 alone but includes anti–CTLA-4 and ICI combinations as well. They found that dendritic cell abundance strongly correlated with irAE risk, followed by TMB among established immunogenomic factors. Consistent with our current study, they also found a significant correlation of irAEs with CD8$^+$ T cells and neoantigen load.

Our study highlights that deconvoluting the role of baseline TIME features across tumor types that may contribute to distinct irAEs will be essential for developing relevant risk stratification and mitigation strategies to improve patient outcomes. Furthermore, the baseline repertoire of the antigen load present on tumors that overlaps with healthy tissue resulting in ICI-induced cross-reactive autoimmunity needs to be further elucidated. Current initiatives such as the National Cancer Institute-Alliance irAE Biorepository study (Alliance 151804)[48] or the South Western Oncology Group S2013: Immune Checkpoint Inhibitor Toxicity study (ClinicalTrials.gov identifier: NCT04871542) will be crucial for further evaluating these biomarker correlations using biobanked samples at baseline and at the time of irAEs.

The link between irAE occurrence and ICI efficacy has been discussed in previous work, including clinical trials. Eggermont et al[50] conducted a post hoc analysis using data from the phase 3 KEYNOTE-054 melanoma trial in the adjuvant setting, comparing pembrolizumab with placebo. They reported a prolonged recurrence-free survival (RFS) in pembrolizumab-treated patients with irAE occurrences compared with those without irAEs after accounting for immortal time bias related to the duration of therapy and treatment exposure. Interestingly, when compared with the placebo arm, RFS reduction in the pembrolizumab arm was more substantial after the onset of an irAE than before an irAE, suggesting a relationship between antigen cross-reactivity for irAEs and ICI outcomes. Others have demonstrated shared antigenicity and TCR clonality between NSCLC biopsies and autoimmune skin lesions in ICI-treated patients with better outcomes,[51] providing evidence for shared mechanisms between mounting a response to ICIs and developing irAEs. The identified biomarkers in our study have been shown to be

successful ICI efficacy indicators. For instance, high INDEL mutation rates were associated with favorable overall and progression-free survival rates in patients with gastric cancer treated with nivolumab,[52] whereas frameshift INDELs were significantly correlated with ICI response across multiple solid tumors.[47,53] Furthermore, we have previously shown that INDELs can complement TMB in predicting outcomes to ICI, especially in microsatellite stable/TMB-low tumors.[54] Similarly, our previous work, alongside other studies, highlighted the potential predictive value of TILs in identifying both response and survival benefit.[44,55,56]

This study serves as a proof of concept but is compounded by multiple limitations. First, irAE frequency and TIME features are tested in separate data sets (FAERS *v* TCGA). Second, neoantigen load and immune cell fractions in the TCGA data are estimated on the basis of RNA sequence data rather than directly measuring on baseline tumors of patients who developed irAEs. In addition, our correlation analysis was limited to TIME features with at least 100 cases, which resulted in variability in included cancers for each analysis. As a result, our composite bivariate model only included cancers with all TIME features (n = 17). Third, the type and association of irAEs in FAERS could be limited to some degree since the complete source documentation and causal attributions for these are not available for cross-checking. Considering that the FAERS database reports reactions (adverse events) and reaction outcomes (seriousness) for each case rather than for each drug, one of the caveats to consider is that we cannot attribute these reactions/outcomes to the ICIs with certainty as they might be the result of other coadministered drugs or the underlying disease in the same patient. This could result in inflation of irAEs to some extent. Finally, for the DFCI cohort, the potential for immortal time bias is high in an observational study reporting irAEs. People are also more likely to have responded to ICIs and might have developed irAEs because of longer ICI exposure. Ideally, one would need to address this with a landmark analysis or a logistic regression modeling for irAEs.

Given the morbidity and mortality associated with irAEs, incorporating a precision immunotherapy approach by accounting for baseline tumor biomarkers, patient risk factors, and pharmacovigilance data could be of immense value.[57] Such an approach of stratified precision immunotherapy could facilitate a balance between limiting toxicity without compromising efficacy by matching the right patient to the right immunotherapy.

AFFILIATIONS

[1]Institute for Computer Science and Control (SZTAKI), Hungarian Research Network (HUN-REN), Budapest, Hungary
[2]Jordan University of Science and Technology, Irbid, Jordan
[3]Lowe Center for Thoracic Oncology, Dana-Farber Cancer Institute, Harvard Medical School, Boston, MA
[4]Yale School of Medicine, New Haven, CT
[5]Brigham and Women's Hospital, Boston, MA
[6]Department of Medicine, Brigham and Women's Hospital, Harvard Medical School, Boston, MA
[7]Departments of Oncological Sciences and Biomedical Informatics, Huntsman Cancer Institute, University of Utah, Salt Lake City, UT
[8]Department of Pathology, Forensic and Insurance Medicine, Semmelweis University, Budapest, Hungary
[9]ImmunoProfile, Brigham and Women's Hospital and Dana-Farber Cancer Institute, Boston, MA
[10]Department of Pathology, Brigham and Women's Hospital, Boston, MA
[11]Department of Probability, Alfred Renyi Institute of Mathematics, The Eötvös Loránd Research Network, Budapest, Hungary
[12]Medical Oncology/TSET Phase 1 Program, Stephenson Cancer Center @The University of Oklahoma, Oklahoma City, OK

CORRESPONDING AUTHOR

Abdul Rafeh Naqash, MD, Medical Oncology/TSET Phase 1 Program, Stephenson Cancer Center @The University of Oklahoma, 800 NE 10th St, Oklahoma City, OK 73104; e-mail: AbdulRafeh-Naqash@ouhsc.edu.

EQUAL CONTRIBUTION

C.K. and H.M.A. contributed equally to this work.

SUPPORT

Supported by the European Union project RRF-2.3.1-21-2022-00004 (C.K.) within the framework of the Artificial Intelligence National Laboratory, Hungary.

AUTHOR CONTRIBUTIONS

Conception and design: Csaba Kerepesi, Elio Adib, Scott J. Rodig, Tibor Bakacs, Abdul Rafeh Naqash
Financial support: Mark M. Awad, Aik Choon Tan
Administrative support: Mark M. Awad, Aik Choon Tan, Abdul Rafeh Naqash
Provision of study materials or patients: Mark M. Awad, Scott J. Rodig
Collection and assembly of data: Csaba Kerepesi, Biagio Ricciuti, Amin H. Nassar, Joao V. Alessi, Federica Pecci, Scott J. Rodig, Mark M. Awad, Aik Choon Tan, Tibor Bakacs, Abdul Rafeh Naqash
Data analysis and interpretation: Csaba Kerepesi, Hassan Mohammed Abushukair, Biagio Ricciuti, Amin H. Nassar, Elio Adib, Joao V. Alessi, Mehrdad Rakaee, Muhammad Zaki Hidayatullah Fadlullah, Scott J. Rodig, Mark M. Awad, Aik Choon Tan, Tibor Bakacs
Manuscript writing: All authors
Final approval of manuscript: All authors
Accountable for all aspects of the work: All authors

AUTHORS' DISCLOSURES OF POTENTIAL CONFLICTS OF INTEREST

The following represents disclosure information provided by authors of this manuscript. All relationships are considered compensated unless otherwise noted. Relationships are self-held unless noted. I = Immediate Family Member, Inst = My Institution. Relationships may not relate to the subject matter of this manuscript. For more information about ASCO's conflict of interest policy, please refer to www.asco.org/rwc or ascopubs.org/po/author-center.

Open Payments is a public database containing information reported by companies about payments made to US-licensed physicians (Open Payments).

Biagio Ricciuti
Honoraria: Targeted Oncology
Consulting or Advisory Role: Regeneron, AstraZeneca, Amgen, Guidepoint Inc

Elio Adib
Employment: Amgen

Scott J. Rodig
Leadership: Immunitas
Stock and Other Ownership Interests: Immunitas
Honoraria: Perkin Elmer, Bristol Myers Squibb
Consulting or Advisory Role: Bristol Myers Squibb
Research Funding: Bristol Myers Squibb, Merck, Affimed Therapeutics, Kite, a Gilead company
Patents, Royalties, Other Intellectual Property: Patent pending for use of anti–galectin-1 antibodies for diagnostic use
Travel, Accommodations, Expenses: Roche, Bristol Myers Squibb

Mark M. Awad
Consulting or Advisory Role: Merck, Pfizer, Bristol Myers Squibb, Foundation Medicine, Novartis, Gritstone Bio, Mirati Therapeutics, EMD Serono, AstraZeneca, Instil Bio, Regeneron, Janssen, Affini-T Therapeutics
Research Funding: Genentech/Roche (Inst), Lilly (Inst), AstraZeneca (Inst), Bristol Myers Squibb (Inst), Amgen (Inst)
Travel, Accommodations, Expenses: Bristol Myers Squibb Foundation
Open Payments Link: https://openpaymentsdata.cms.gov/physician/1127368

Aik Choon Tan
Employment: Bristol Myers Squibb/Celgene/Juno
Stock and Other Ownership Interests: Bristol Myers Squibb/Celgene/Juno

Tibor Bakacs
Employment: PRET Therapeutics Ltd
Stock and Other Ownership Interests: PRET Therapeutics Ltd
Patents, Royalties, Other Intellectual Property: Low-dose immune checkpoint blockade in metastatic cancer, US Patent 11,161,903

Abdul Rafeh Naqash
This author is a Social Media Editor and Podcast Host for *JCO Precision Oncology*. Journal policy recused the author from having any role in the peer review of this manuscript.

No other potential conflicts of interest were reported.

REFERENCES

1. Ma W, Xue R, Zhu Z, et al: Increasing cure rates of solid tumors by immune checkpoint inhibitors. Exp Hematol Oncol 12:10, 2023
2. Khoja L, Day D, Wei-Wu Chen T, et al: Tumour- and class-specific patterns of immune-related adverse events of immune checkpoint inhibitors: A systematic review. Ann Oncol 28:2377-2385, 2017
3. Sato K, Akamatsu H, Murakami E, et al: Correlation between immune-related adverse events and efficacy in non-small cell lung cancer treated with nivolumab. Lung Cancer 115:71-74, 2018
4. Sugano T, Seike M, Saito Y, et al: Immune checkpoint inhibitor-associated interstitial lung diseases correlate with better prognosis in patients with advanced non-small-cell lung cancer. Thorac Cancer 11:1052-1060, 2020
5. Schulz GB, Rodler S, Szabados B, et al: Safety, efficacy and prognostic impact of immune checkpoint inhibitors in older patients with genitourinary cancers. J Geriatr Oncol 11:1061-1066, 2020
6. Huang L, Li L, Zhou Y, et al: Clinical characteristics correlate with outcomes of immunotherapy in advanced non-small cell lung cancer. J Cancer 11:7137-7145, 2020
7. Akamatsu H, Murakami E, Oyanagi J, et al: Immune-related adverse events by immune checkpoint inhibitors significantly predict durable efficacy even in responders with advanced non-small cell lung cancer. Oncologist 25:e679-e683, 2020
8. Zhong L, Wu Q, Chen F, et al: Immune-related adverse events: Promising predictors for efficacy of immune checkpoint inhibitors. Cancer Immunol Immunother 70:2559-2576, 2021
9. Xu S, Lai R, Zhao Q, et al: Correlation between immune-related adverse events and prognosis in hepatocellular carcinoma patients treated with immune checkpoint inhibitors. Front Immunol 12: 794099, 2021
10. Wang D, Chen C, Gu Y, et al: Immune-related adverse events predict the efficacy of immune checkpoint inhibitors in lung cancer patients: A meta-analysis. Front Oncol 11:631949, 2021
11. Paderi A, Giorgione R, Giommoni E, et al: Association between immune related adverse events and outcome in patients with metastatic renal cell carcinoma treated with immune checkpoint inhibitors. Cancers (Basel) 13:860, 2021
12. Kazama S, Morimoto R, Kimura Y, et al: Prognostic impact of immune-related adverse events on patients with and without cardiovascular disease: A retrospective review. Cardiooncology 7:26, 2021
13. Kato T, Nagahara A, Kawamura N, et al: The prognostic impact of immune-related adverse events in metastatic renal cell carcinoma patients treated with nivolumab: A real-world multi-institutional retrospective study. Int J Clin Oncol 26:954-961, 2021
14. Dimitriou F, Staeger R, Ak M, et al: Frequency, treatment and outcome of immune-related toxicities in patients with immune-checkpoint inhibitors for advanced melanoma: Results from an institutional database analysis. Cancers (Basel) 13:2931, 2021
15. Bai R, Li L, Chen X, et al: Correlation of peripheral blood parameters and immune-related adverse events with the efficacy of immune checkpoint inhibitors. J Oncol 2021:9935076, 2021
16. Bai R, Chen N, Chen X, et al: Analysis of characteristics and predictive factors of immune checkpoint inhibitor-related adverse events. Cancer Biol Med 18:1118-1133, 2021
17. Ando T, Ueda A, Ogawa K, et al: Prognosis of immune-related adverse events in patients with advanced gastric cancer treated with nivolumab or pembrolizumab: A multicenter retrospective analysis. In Vivo 35:475-482, 2021
18. Abdihamid O, Omar A, Rugambwa T: Defining the correlation between immune-checkpoint inhibitors-related adverse events and clinical outcomes: A narrative review. Ecancermedicalscience 15: 1314, 2021
19. Ng KYY, Tan SH, Tan JJE, et al: Impact of immune-related adverse events on efficacy of immune checkpoint inhibitors in patients with advanced hepatocellular carcinoma. Liver Cancer 11:9-21, 2022
20. Kuzmanovszki D, Kiss N, Tóth B, et al: Anti-PD-1 monotherapy in advanced melanoma-real-world data from a 77-month-long retrospective observational study. Biomedicines 10:1737, 2022
21. Alomari M, Al Ashi S, Chadalavada P, et al: Gastrointestinal toxicities of immune checkpoint inhibitors are associated with enhanced tumor responsiveness and improved survival. Gastroenterol Res 15:56-66, 2022
22. Bastacky ML, Wang H, Fortman D, et al: Immune-related adverse events in PD-1 treated melanoma and impact upon anti-tumor efficacy: A real world analysis. Front Oncol 11:749064, 2021
23. Socinski MA, Jotte RM, Cappuzzo F, et al: Association of immune-related adverse events with efficacy of atezolizumab in patients with non-small cell lung cancer: Pooled analyses of the phase 3 IMpower130, IMpower132, and IMpower150 randomized clinical trials. JAMA Oncol 9:527-535, 2023
24. Hara Y, Baba Y, Toihata T, et al: Immune-related adverse events and prognosis in patients with upper gastrointestinal cancer treated with nivolumab. J Gastrointest Oncol 13:2779-2788, 2022
25. Amoroso V, Gallo F, Alberti A, et al: Immune-related adverse events as potential surrogates of immune checkpoint inhibitors' efficacy: A systematic review and meta-analysis of randomized studies. ESMO Open 8:100787, 2023
26. Zhang YC, Zhu TC, Nie RC, et al: Association between early immune-related adverse events and survival in patients treated with PD-1/PD-L1 inhibitors. J Clin Med 12:736, 2023

27. Cao R, Wu C, Lv Y, et al: Correlation between immune-related adverse events and treatment efficacy of anti-PD1 immunotherapy in patients with esophageal squamous cell carcinoma. Oncol Lett 25:55, 2023
28. Sung C, An J, Lee S, et al: Integrative analysis of risk factors for immune-related adverse events of checkpoint blockade therapy in cancer. Nat Cancer 4:844-859, 2023
29. Conroy M, Naidoo J: Immune-related adverse events and the balancing act of immunotherapy. Nat Commun 13:392, 2022
30. Groha S, Alaiwi SA, Xu W, et al: Germline variants associated with toxicity to immune checkpoint blockade. Nat Med 28:2584-2591, 2022
31. Rieder D, Trajanoski Z: Checking immunotoxicity risks of checkpoint blockade. Nat Cancer 4:779-780, 2023
32. Zhang L, Shi Y, Han X: Immunogenomic correlates of immune-related adverse events for anti-programmed cell death 1 therapy. Front Immunol 13:1032221, 2022
33. Kerepesi C, Bakacs T, Moss RW, et al: Significant association between tumor mutational burden and immune-related adverse events during immune checkpoint inhibition therapies. Cancer Immunol Immunother 69:683-687, 2020
34. Bomze D, Hasan Ali O, Bate A, et al: Association between immune-related adverse events during anti–PD-1 therapy and tumor mutational burden. JAMA Oncol 5:1633-1635, 2019
35. Ricciuti B, Naqash AR, Naidoo J, et al: Association between immune-related adverse events and clinical outcomes to programmed cell death protein 1/programmed death-ligand 1 blockade in SCLC. JTO Clin Res Rep 1:100074, 2020
36. Thorsson V, Gibbs DL, Brown SD, et al: The immune landscape of cancer. Immunity 51:411-412, 2019
37. FDA Adverse Event Reporting System (FAERS) Quarterly Data Extract Files. https://fis.fda.gov/extensions/FPD-QDE-FAERS/FPD-QDE-FAERS.html
38. Reference deleted
39. Alessi JV, Ricciuti B, Wang X, et al: Impact of TMB/PD-L1 expression and pneumonitis on chemoradiation and durvalumab response in stage III NSCLC. Nat Commun 14:4238, 2023
40. Feng Z, Puri S, Moudgil T, et al: Multispectral imaging of formalin-fixed tissue predicts ability to generate tumor-infiltrating lymphocytes from melanoma. J Immunother Cancer 3:47, 2015
41. Bogusz AM, Baxter RH, Currie T, et al: Quantitative immunofluorescence reveals the signature of active B-cell receptor signaling in diffuse large B-cell lymphoma. Clin Cancer Res 18:6122-6135, 2012
42. Wang DY, Salem J, Cohen JV, et al: Fatal toxic effects associated with immune checkpoint inhibitors: A systematic review and meta-analysis. JAMA Oncol 4:1721-1728, 2018
43. Reference deleted
44. Rakaee M, Adib E, Ricciuti B, et al: Association of machine learning–based assessment of tumor-infiltrating lymphocytes on standard histologic images with outcomes of immunotherapy in patients with NSCLC. JAMA Oncol 9:51-60, 2023
45. Xie N, Shen G, Gao W, et al: Neoantigens: Promising targets for cancer therapy. Signal Transduct Target Ther 8:9, 2023
46. Morad G, Helmink BA, Sharma P, et al: Hallmarks of response, resistance, and toxicity to immune checkpoint blockade. Cell 184:5309-5337, 2021
47. Turajlic S, Litchfield K, Xu H, et al: Insertion-and-deletion-derived tumour-specific neoantigens and the immunogenic phenotype: A pan-cancer analysis. Lancet Oncol 18:1009-1021, 2017
48. Kozono DE, Sharon E, Le-Rademacher J, et al: Alliance A151804: Establishment of a national biorepository to advance studies of immune-related adverse events. Journal for ImmunoTherapy of Cancer 10, A1290-A1291, 2022
49. Reference deleted
50. Eggermont AMM, Kicinski M, Blank CU, et al: Association between immune-related adverse events and recurrence-free survival among patients with stage III melanoma randomized to receive pembrolizumab or placebo: A secondary analysis of a randomized clinical trial. JAMA Oncol 6:519-527, 2020
51. Berner F, Bomze D, Diem S, et al: Association of checkpoint inhibitor–induced toxic effects with shared cancer and tissue antigens in non–small cell lung cancer. JAMA Oncol 5:1043-1047, 2019
52. Kim HD, Ryu MH, Park YS, et al: Insertion-deletion rate is a qualitative aspect of the tumor mutation burden associated with the clinical outcomes of gastric cancer patients treated with nivolumab. Gastric Cancer 25:226-234, 2022
53. Chae YK, Viveiros P, Lopes G, et al: Clinical and immunological implications of frameshift mutations in lung cancer. J Thorac Oncol 14:1807-1817, 2019
54. Florou V, Floudas CS, Maoz A, et al: Real-world pan-cancer landscape of frameshift mutations and their role in predicting responses to immune checkpoint inhibitors in cancers with low tumor mutational burden. J Immunother Cancer 11:e007440, 2023
55. Park S, Ock CY, Kim H, et al: Artificial intelligence-powered spatial analysis of tumor-infiltrating lymphocytes as complementary biomarker for immune checkpoint inhibition in non-small-cell lung cancer. J Clin Oncol 40:1916-1928, 2022
56. Gataa I, Mezquita L, Rossoni C, et al: Tumour-infiltrating lymphocyte density is associated with favourable outcome in patients with advanced non-small cell lung cancer treated with immunotherapy. Eur J Cancer 145:221-229, 2021
57. Desai A, Subbiah V: Rationalizing rules for immunotherapy combination trials: About time for precision immunotherapy. Cancer 129:11-14, 2023
58. Bate A, Evans SJ: Quantitative signal detection using spontaneous ADR reporting. Pharmacoepidemiol Drug Saf 18:427-436, 2009